Composite Right/Left-Handed Leaky-Wave Antennas for Wide-Angle Beam Scanning with Flexibly Chosen Frequency Range

Debabrata K. Karmokar, *Member, IEEE,* Y. Jay Guo, *Fellow, IEEE,* Shu-Lin Chen, *Student Member, IEEE,* and Trevor S. Bird, *Life Fellow, IEEE*

***Abstract*—A composite right/left-handed (CRLH) leaky-wave antenna (LWA) can effectively scan the radiation beam from backward to forward direction. However, in most cases a large range of frequency sweep is required to achieve a wide-angle beam scan, which could limit their applications. An in-depth study is conducted on an equivalent circuit model for a CRLH LWA unit cell to find the controlling parameters on the frequency sweeping range. A systematic design guideline is given for a CRLH LWA for a wide-angle beam scan in a flexibly chosen frequency range. It is shown that beam scanning by sweeping frequency in a target range can be achieved by systematically designing the unit cell parameters. To verify our approach a novel CRLH unit cell is developed and used to design an LWA for a wide-angle beam scan in a narrow frequency range. Finally, the concept is validated through realization of the antenna and its measurement. The measured results show that the antenna prototype can scan its beam from -56° to $+51^\circ$ when frequency sweeps from 5.1 to 6.11 GHz (i.e., 18.02% of fractional bandwidth).**

***Keywords*—Beam scanning, broadside, backward, composite right/left-handed (CRLH), forward, frequency range, leaky-wave antenna (LWA).**

I. Introduction

THE field of leaky-wave antennas (LWAs) has a long history, started back in the 1940s when a waveguide-based leaky structure was introduced [1]. In the next few decades various LWAs based on a waveguide structure were developed [2], [3]. As an another type, LWAs based on microstrip technology, were developed by W. Menzel in the late 1970s [4]. The field of LWAs has gained significant research interest because of their beam scanning capabilities and potential applications such as frequency scanning radars, missiles, aircraft, surveillance, point-to-point communications, etc. [5]–[7]. Due to the structural simplicity, i.e., planar low-profile configuration and without requiring a complicated feed network, they can be integrated easily with microwave and millimeter wave circuits [8]–[12].

It is known that, for LWAs at a particular frequency f, the beam direction θ of the leaky modes is determined by the phase constant (β) and the free-space wavenumber (k_0) from the following approximate expression [13]:

$$\theta(f) \approx \sin^{-1}\Big[\frac{\beta(f)}{k_0(f)}\Big], \tag{1}$$

where θ is the angle between the main beam and the broadside direction. In (1) we see that both β and k_0 are frequency dependent and hence the radiation beam direction changes with the source frequency [12], [14].

In terms of the beam-scanning capability, in most cases, especially for uniform and periodic LWAs, they are unable to scan continuously through broadside. This happens due to an open stopband (OSB), when reflection occurs from the unit cells instead of radiation, restricting broadside radiation [15], [16]. Continuous beam scanning through broadside is challenging and has gained significant attention in recent decades [17]–[22]. Some methods have been proposed to overcome this limitation. One method is to achieve radiation from a higher-mode harmonic, e.g., the $n = -1$ spatial harmonic of a periodic LWA structure, to scan the beam continuously through broadside by suppressing the OSB [18]–[20]. Use of an artificial transmission line called composite right/left-handed (CRLH) structure in LWA design is another effective and widely used method to realize continuous backward to forward beam scanning [22]–[26]. It can be seen from (1) that the beam points in the backward directions, i.e., θ values are negative, when β is negative. Artificially created transmission lines can support forward (right-handed, RH) and backward (left-handed, LH) wave propagation. They can have a propagation constant that is negative, zero and positive depending on the design and due to this exceptional properties they have been used in various antenna applications [27]–[31]. An LWA made out of such a structure is called a CRLH LWA. Nonetheless, a balanced condition is required for beam scanning continuously through the broadside using such a structure [26].

To create a CRLH structure, the LH properties are artificially introduced in a structure while the RH properties occur inherently in it [22], [30]. In the case of a CRLH LWA the properties of the antenna structure change from LH, when

Manuscript received ——-. This work was supported by the Australian Research Council (ARC) under a Discovery Project (DP) (Grant no. 160102219). *(Corresponding author: Shu-Lin Chen.)*

D. K. Karmokar was with the Global Big Data Technologies Center (GBDTC), University of Technology Sydney (UTS), Ultimo, NSW 2007, Australia. He is now with the School of Engineering, Faculty of Science and Engineering, Macquarie University, Sydney, NSW 2109, Australia (e-mail: dkkarmokar@ieee.org).

Y. J. Guo, S.-L. Chen, and T. S. Bird are with the Global Big Data Technologies Centre (GBDTC), Faculty of Engineering and Information Technology, University of Technology Sydney, Ultimo, NSW 2007, Australia (e-mail: jay.guo@uts.edu.au; shulin.chen@uts.edu.au; ts.bird@ieee.org).

$\beta < 0$ (backward radiation), to RH, when $\beta > 0$ (forward radiation), as the frequency increases. The antenna radiates towards the broadside in its balanced condition, i.e., at the transition point [32], [33]. The period of a CRLH structure is small compared to a wavelength, and this type of structure normally falls into the quasi-uniform category. The radiation occurs by the fundamental harmonic (n = 0 harmonic) from a CRLH structure [15].

An LWA based on a CRLH structure, realizing continuous beam scanning through broadside, was reported in 2002 [24]. Because of the exceptional properties of the CRLH structure, they have been widely used in LWA design and various advancements have been made, e.g., cross-polarization reduction, broadside radiation improvement, leaky wave radiation from two frequency bands, enhancement of scanning range etc. [34]–[42]. Despite these advancements there is still one remaining issue unresolved: how to design a CRLH LWA for a wide-angle beam scan in a desired frequency range. Usually, a broad range of frequency sweep is required to realize a wide-angle beam scan for CRLH LWAs. For practical antenna applications, however, in most of the cases the allocated frequency band is normally predefined [43]–[45]. Thus fitting the frequency sweep of the LWAs to the required ones is of high importance.

In this paper, the properties of the classic CRLH LWA unit cell are studied in detail to find the controlling parameters on the frequency sweeping range of a CRLH LWA. A systematic design procedure with a prescribed frequency range is presented to assist designers to produce an antenna with acceptable performance. Then, following the design guideline, a novel unit cell is proposed, analyzed using unit cell dispersion and an equivalent circuit model, and subsequently used to design a CRLH LWA for operation in a desired frequency range. The complete antenna structure is further analyzed to show its radiation and beam scanning performance. Finally, the proposed antenna is fabricated and measured to validate the design concept.

Our paper is organized as follows. Section II presents an in-depth study on the equivalent circuit model for a CRLH transmission line structure to observe the effect of the circuit parameters on the frequency range. A systematic guideline for designing a CRLH LWA for beam scanning by sweeping a desired frequency range is also outlined here. Section III describes a novel unit cell design following the guideline in Section II and subsequently a complete CRLH LWA operating in a desired frequency range. Measured results of the antenna prototype are also given in this section. A short discussion on the findings of our study together with a comparison between the proposed antenna in this paper and reference antennas are given in Section IV, and finally Section V concludes the paper.

II. Theory

We commence from the equivalent circuit model of a CRLH LWA unit cell. Figs. 1(a) and (b) show the equivalent circuit model for a conventional (right-handed) transmission line and a CRLH LWA unit cell, respectively. The well-known conventional transmission line equivalent circuit consists of

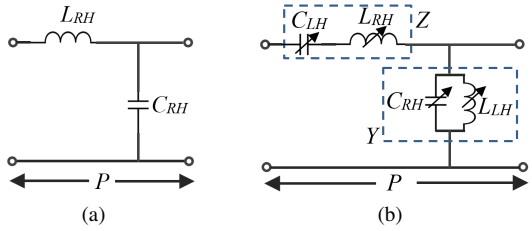

Fig. 1. Equivalent unit cell circuit model. (a) Conventional (or right-handed) transmission line. (b) Composite right/left-handed (CRLH) transmission line. The variable equivalent circuit components represent our study on the circuit model for different sets of circuit parameter values.

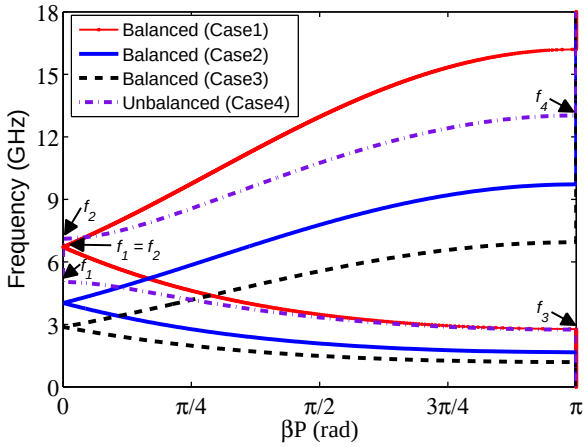

Fig. 2. Dispersion diagram obtained by analyzing the equivalent circuit model of a CRLH unit cell in Fig. 1(b). The circuit parameters are: Case1: L_{RH} = 0.75 nH, L_{LH} = 0.75 nH, C_{RH} = 0.75 pF and C_{LH} = 0.75 pF; Case2: L_{RH} = 1.25 nH, L_{LH} = 1.25 nH, C_{RH} = 1.25 pF and C_{LH} = 1.25 pF; Case3: L_{RH} = 1.75 nH, L_{LH} = 1.75 nH, C_{RH} = 1.75 pF and C_{LH} = 1.75 pF; Case4: L_{RH} = 1 nH, L_{LH} = 1 nH, C_{RH} = 1 pF and C_{LH} = 0.5 pF.

a RH inductance (inductance in the series branch, i.e., L_{RH}) and a RH capacitance (capacitance in the shunt branch, i.e., C_{RH}) as shown in Fig. 1(a). On the other hand, the equivalent circuit model of a CRLH unit cell [Fig. 1(b)] consists of a series impedance, a combination of an inductor and a capacitor connected in series, and a shunt combination of an inductor and a capacitor [46]. As mentioned earlier, to achieve LH properties, a series capacitor (capacitance of C_{LH}) and a shunt inductor (inductance of L_{LH}) are added artificially.

To disclose the mechanism behind flexible control of the frequency range for wide-angle beam scanning, the study was conducted on the unit cell equivalent circuit model. The analysis is carried out using MATLAB, and provides an appropriate guideline to design a unit cell of a CRLH LWA with a desired frequency-sweeping range for a wide-angle beam scan.

For a transmission line made out of cascaded unit cells with period *P* and infinite length, the Bloch-Floquet theorem can be applied to find the dispersion relation and expressed in terms of the transmission matrix coefficient of the unit cell as [35], [47]

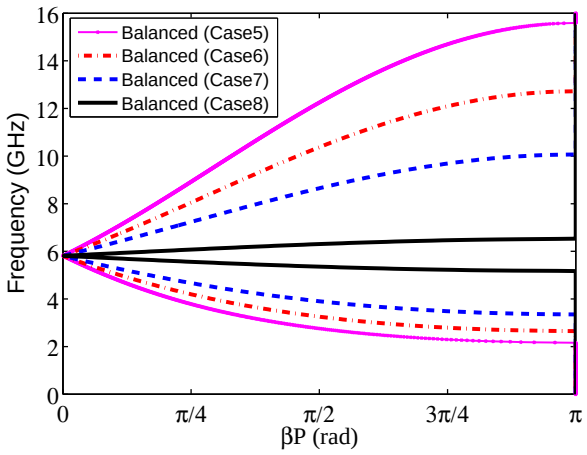

Fig. 3. Dispersion diagram obtained by analyzing the equivalent circuit model of a CRLH unit cell in Fig. 1(b). The circuit parameters are: Case5: L_{RH} = 0.75 nH, L_{LH} = 1.0 nH, C_{RH} = 0.75 pF and C_{LH} = 1.0 pF; Case6: L_{RH} = 1 nH, L_{LH} = 0.75 nH, C_{RH} = 1 pF and C_{LH} = 0.75 pF; Case7: L_{RH} = 1.5 nH, L_{LH} = 0.5 nH, C_{RH} = 1.5 pF and C_{LH} = 0.5 pF; Case8: L_{RH} = 7.5 nH, L_{LH} = 0.1 nH, C_{RH} = 7.5 pF and C_{LH} = 0.1 pF.

$$\beta = \frac{1}{P}\cos^{-1}\Big(\frac{A+D}{2}\Big). \tag{2}$$

The coefficients A and D can be obtained from the unit cell transmission matrix by multiplying the element matrices given below:

$$A = 1 + YZ \quad \text{and} \quad D = 1 \tag{3}$$

The impedance Z and admittance Y can be easily calculated from the equivalent circuit model in Fig. 1(b) and hence we get

$$A + D = 2 + \frac{L_{RH}}{L_{LH}} + \frac{C_{RH}}{C_{LH}} - \omega^2 L_{RH}C_{RH} - \frac{1}{\omega^2 L_{LH}C_{LH}} \tag{4}$$

In (4), ω is the angular frequency, i.e., $\omega = 2\pi f$.

The dispersion diagram for the equivalent circuit can be obtained using (2) as shown in Fig. 2. For continuous backward-to-forward beam scanning, without any bandgap, as shown by 'Case1' in Fig. 2, a balanced condition is required as given below [48]:

$$\frac{L_{RH}}{L_{LH}} = \frac{C_{RH}}{C_{LH}} \tag{5}$$

which is obtained from (2) with $\beta = 0$, giving $f_1 = f_2$ where

$$f_1 = \min\Big(\frac{1}{2\pi\sqrt{L_{RH}C_{LH}}}, \frac{1}{2\pi\sqrt{L_{LH}C_{RH}}}\Big)$$
$$f_2 = \max\Big(\frac{1}{2\pi\sqrt{L_{RH}C_{LH}}}, \frac{1}{2\pi\sqrt{L_{LH}C_{RH}}}\Big) \tag{6}$$

However, the structure is unbalanced when $f_1 \neq f_2$.

By solving (2) for $\beta = \pi/P$ the cutoff frequencies f_3 and f_4 are obtained below:

$$f_3 = \frac{1}{4\pi L_{RH}C_{RH}L_{LH}C_{LH}} \times \{2L_{RH}C_{RH}L_{LH}C_{LH} \times (4L_{LH}C_{LH} + L_{LH}C_{RH} + L_{RH}C_{LH} - \sqrt{M})\}^{1/2} \tag{7}$$

where

$$M = L_{RH}^2C_{LH}^2 + L_{LH}^2C_{RH}^2 + 16L_{LH}^2C_{LH}^2 + 8L_{LH}^2C_{LH}C_{RH} + 8L_{LH}C_{LH}^2L_{RH} - 2L_{LH}C_{LH}C_{RH}L_{RH} \tag{8}$$

and

$$f_4 = \frac{1}{4\pi L_{RH}C_{RH}L_{LH}C_{LH}} \times \{2L_{RH}C_{RH}L_{LH}C_{LH} \times (4L_{LH}C_{LH} + L_{LH}C_{RH} + L_{RH}C_{LH} + \sqrt{M})\}^{1/2} \tag{9}$$

A study is conducted for several conditions based on the equivalent circuit parameters as shown in Figs. 2 and 3. The dispersion diagrams were obtained using (2) for different sets of circuit parameters to observe the characteristics of the unit cell in each case. The solution of (2) for two different conditions, i.e., $\beta = 0$ and $\beta = \pi/P$, also makes it convenient to determine the frequency sweep range and the transition frequency. The cutoff frequencies are determined easily using (7) and (9), and the transition frequency from (6). A summary of the study on a CRLH LWA frequency range for a wide-angle beam scan is given below.

i A simultaneous increase of all the parameter values moves the dispersion curves to lower frequencies ('Case2' and 'Case3' in Fig. 2 compared to 'Case1'). When the balanced condition (5) is not satisfied (Case4), a bandgap is created between two leaky regions. The bandgap can also be calculated using (6).

ii Reducing L_{RH} and C_{RH} while simultaneously increasing L_{LH} and C_{LH} increases the frequency range significantly ('Case5' in Fig. 3).

iii Increasing L_{RH} and C_{RH} and simultaneously decreasing L_{LH} and C_{LH} reduces the frequency range significantly ('Case6', 'Case7', and 'Case8' in Fig. 3).

It is worth noting that, in points (ii) and (iii) above, to maintain the same transition frequency point while increasing or decreasing the frequency range (see Fig. 3), the ratios of the increment and decrement of the circuit parameter values should be the same. This means that, if the RH circuit parameter values are increased N times, LH parameter values should be reduced $1/N$ times (for frequency range reduction) and vice versa (for increasing frequency range). For example, if L_{RH} and C_{RH} increase three times, L_{LH} and C_{LH} need to be reduced to one-third to maintain the same transition point.

From the above study a design can be undertaken for a desired frequency range operation. A systematic procedure for designing such an antenna in a desired frequency range is outlined below:

1) Let the cutoff frequencies for a desired operating frequency range be from f_3 (lower) to f_4 (higher).

2) For the desired values of f_3 and f_4, the values of the circuit parameters L_{RH}, C_{RH}, L_{LH}, and C_{LH} can be calculated from (7) - (9). Now, using the circuit parameter values, the dispersion can be obtained using (2).
3) From the above circuit parameters values and using microstrip line circuit parameter calculation formulas [49]–[51], i.e., formulas to calculate the patch inductance, gap capacitance, via inductance etc., the dimensions of a physical unit cell can be approximately determined.
4) By simulating the unit cell using a commercial software and observing the dispersion behavior, and optimizing its parameters (if required) the final dispersion diagram can be obtained and hence a unit cell can be designed. As the antenna operates in the fast-wave region the frequency of operation is determined by β and k_0, i.e., the frequency range is determined by $\beta < k_0$.
5) The next step is to use the unit cell to design a complete CRLH LWA with an appropriate feed line, and a full-wave simulation would provide the radiation and scanning performance of the antenna structure.
6) If the operating frequency range is slightly different from the desired ones, by following the previous steps 1 to 5 above and properly tuning the values of the circuit parameters and iterating these steps, the targeted operating frequency range can be readjusted.

The above summary provides an appropriate guideline for designing a CRLH LWA for wide-angle beam scanning by sweeping frequency in a desired range. Note that if the antenna is intended for a very narrow operating band the scan range will reduce unless the unit cell is highly dispersive. The study presented here will be used in the next section to design a CRLH LWA that can support a wide-angle beam scan in a narrow frequency range.

III. A CRLH LWA Design for Wide-Angle Beam Scan in a Narrow Frequency Range

Following the previous study, a CRLH LWA is designed for scanning the main beam over a wide angle with a narrow frequency range. Although the antenna discussed here can cover the whole 5 GHz WLAN IEEE 802.11n frequency band, following the guidelines given in the previous section one can design an antenna for other real-world application frequency ranges. From our study in Section II we see that to reduce the frequency range we need to increase the right-handed inductance (L_{RH}) and the right-handed capacitance (C_{RH}) and simultaneously reduce the left-handed inductance (L_{LH}) and the left-handed capacitance (C_{LH}). In a unit cell L_{RH} and C_{RH} can be easily increased by increasing the size of the patch, C_{LH} can be decreased by introducing more left-handed capacitance in series, and L_{LH} can be reduced by using more inductors in parallel. In this section a novel unit cell is designed followed by a new CRLH LWA in which a reduced range of frequency sweep is achieved for a wide-angle beam scan.

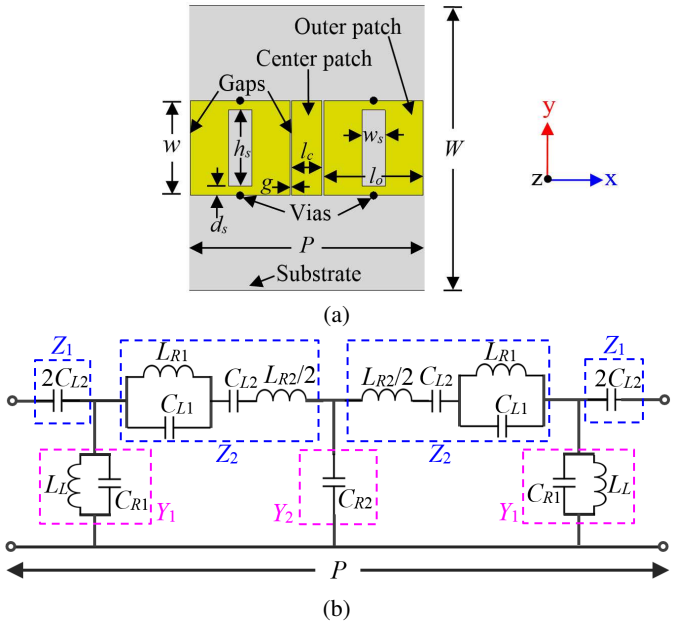

Fig. 4. (a) Unit Cell of a CRLH LWA with reduced frequency sweep. (b) Approximate equivalent circuit model for the CRLH LWA unit cell in Fig. 4(a). The circuit parameters are: L_{R1} = 2.45 nH, C_{R1} = 1.43 pF, C_{L1} = 0.15 pF, L_L = 0.41 nH, L_{R2} = 0.51 nH, C_{R2} = 0.41 pF and C_{L2} = 0.47 pF.

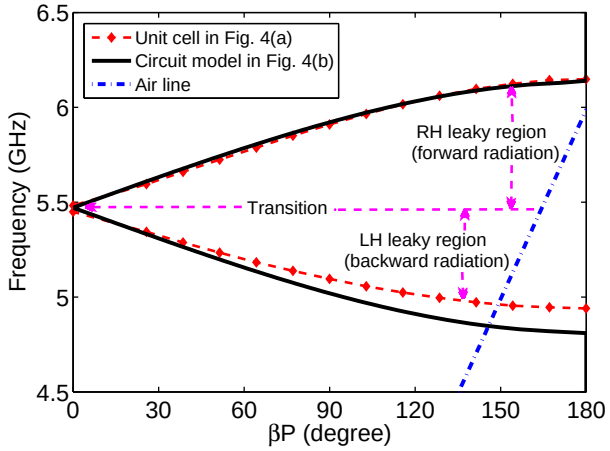

Fig. 5. Dispersion diagram of the CRLH LWA unit cell in Fig. 4(a) and the equivalent circuit model in Fig. 4(b).

A. Unit Cell Design

The unit cell was designed by following the steps given in Section II. Fig. 4(a) shows the top view of the unit cell. Rogers RT5870 substrate with a thickness of 1.575 mm is used to design the unit cell and antenna. The dielectric constant (ε_r) and loss tangent (tanδ) of the substrate are 2.33 and 0.0012, respectively. It is well known that the equivalent capacitance and inductance decrease when they are in series and parallel, respectively, and vice versa. An enlarged unit cell is considered to increase the RH inductance and RH capacitance. In case of series LH capacitance, it depends on the gap when other

parameters are fixed and decreases as the gap increases. The equivalent capacitance obviously decreases when they are connected in series. In our design, we use this concept to reduce the left-handed capacitance by using two gap capacitors and two slot capacitors inside the unit cell together with a gap at each side as shown in Fig. 4(a). In order to reduce the left-handed inductance, four vias are used in each unit cell. The parameters of the unit cell are then optimized using a parameter analysis in CST Microwave Studio to achieve the balanced condition.

The unit cell in Fig. 4(a) can be divided into three parts. The middle part consists of a patch called the center patch [in Fig. 4(a)]. The length (l_c) and width (w) of the patch are 3.25 and 10 mm, respectively. There are two more patches, the outer patches in Fig. 4(a), one at each side of the center patch. The width of the outer patch is the same as the width of the center patch and its length (l_o) is 10.6 mm. There is a 0.2 mm gap (g) between the outer and the center patches. Both edges of the outer patch are shorted to the ground plane by two vias and the radius of each via is 0.4 mm. As mentioned before, there is a slot at the center of the outer patch. The dimensions of the slot are 8 mm $\times$ 2.5 mm ($h_s \times w_s$). The length (P) and width (W) of the substrate are 25.05 and 30 mm, respectively.

The CST eigenmode solver is used to obtain the dispersion diagram for the unit cell illustrated in Fig. 4(a) and this is shown in Fig. 5. Note that, the 'Air line' in Fig. 5 is given by k_0P. From the dispersion diagram we see that a narrow range of frequency sweep is required to achieve a wide-angle beam scan. Now, an equivalent circuit model for the unit cell is developed to verify our study. Fig. 4(b) represents the simplified circuit model for the unit cell in Fig. 4(a). The equivalent circuit is modeled considering the physical parameters of the unit cell. The unit cell is symmetric from the center, looking at the left and right sides from the center patch in Fig. 4(a), and the equivalent circuit is designed accordingly. In the equivalent circuit model C_{R2} represents the capacitance formed between the center patch and the ground plane, L_{R2} is the inductance of the center patch, L_{R1} is the inductance of the outer patch, C_{L1} is the slot capacitance in the outer patch, C_{L2} is the equivalent capacitance formed in the gaps between two patches, C_{R1} is the capacitance formed between the outer patch and the ground plane, and L_L is the equivalent inductance of the vias at each side of the center patch.

The transmission matrix for the equivalent circuit model in Fig. 4(b) can be obtained by multiplying the element matrices which is given in (10) below:

$$\begin{bmatrix} A & B \\ C & D \end{bmatrix} = \begin{bmatrix} 1 & Z_1 \\ 0 & 1 \end{bmatrix} \times \begin{bmatrix} 1 & 0 \\ Y_1 & 1 \end{bmatrix} \times \begin{bmatrix} 1 & Z_2 \\ 0 & 1 \end{bmatrix} \times \begin{bmatrix} 1 & 0 \\ Y_2 & 1 \end{bmatrix} \times \begin{bmatrix} 1 & Z_2 \\ 0 & 1 \end{bmatrix} \times \begin{bmatrix} 1 & 0 \\ Y_1 & 1 \end{bmatrix} \begin{bmatrix} 1 & Z_1 \\ 0 & 1 \end{bmatrix} \quad (10)$$

After multiplying all the element matrices the transmission matrix coefficients A and D are obtained as follows:

$$A = D = 1 + 2Y_1Z_1 + Y_2Z_2 + 2Y_1Z_1Y_2Z_2 + Y_2Z_1 + 2Y_1Z_2 + 2Y_1^2Z_1Z_2 + Y_1Y_2Z_2^2 + Y_1^2Z_1Y_2Z_2^2 \quad (11)$$

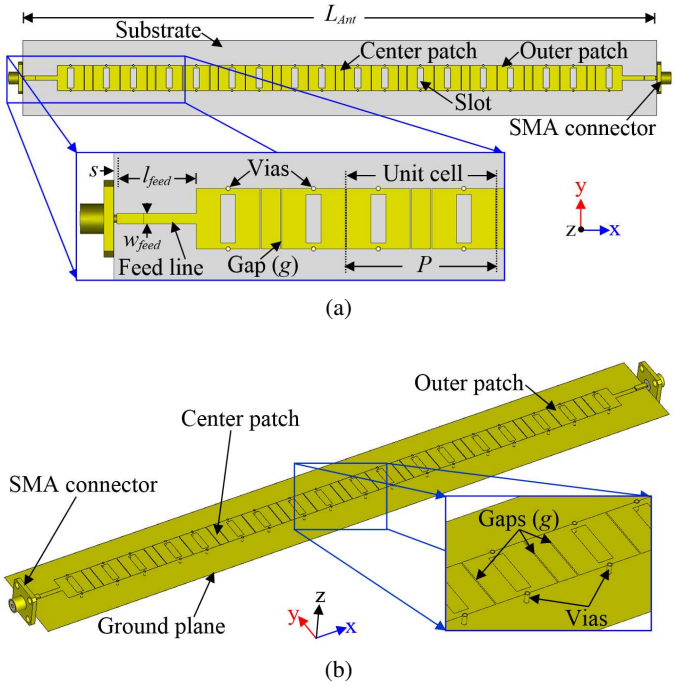

Fig. 6. CRLH LWA for wide-angle beam scanning with reduced frequency sweep. (a) Top view. (b) Substrate-omitted perspective view.

where,

$$Z_1 = \frac{1}{2j\omega C_{L2}},$$
$$Z_2 = j\frac{(1-\omega^2 L_{R1}C_{L1})(\omega^2 L_{R2}C_{L2}-2)+2\omega^2 L_{R1}C_{L2}}{2\omega C_{L2}(1-\omega^2 L_{R1}C_{L1})},$$
$$Y_1 = \frac{1-\omega^2 L_L C_{R1}}{j\omega L_L}, \quad \text{and} \quad Y_2 = j\omega C_{R2}. \quad (12)$$

Now, the phase constant β can be calculated from (2) by using the values of A and D from (11). The values of the equivalent circuit parameters are given in the Fig. 4 caption. The circuit parameter values were initially calculated approximately using the microstrip line circuit parameter calculation formulas [49]–[51] as given below:

$$L_{Right} \approx \mu_r\mu_0 hl/w \quad (13)$$

$$L_{Left} \approx 0.2h\Big(\ln\frac{4h}{d}+1\Big)\times 10^{-6} \quad (14)$$

$$C_{Right} \approx \varepsilon_r\varepsilon_0 wl/h \quad (15)$$

$$C_{Left} \approx 0.5he^{-\frac{1.86g}{h}}\Big[1+4.19\Big(1-e^{-0.785\sqrt{\frac{h}{w}}}\Big)\Big]Q \quad (16)$$

where,

$$Q \approx 0.046\big[0.03+\big(\frac{w}{h}\big)^{1.23}\big](0.272+0.07\varepsilon_r)\times 10^{-9}. \quad (17)$$

In (13) – (17), ε_r, ε_0, μ_r and μ_0 are the substrate relative permittivity, the permittivity of free space, the substrate relative

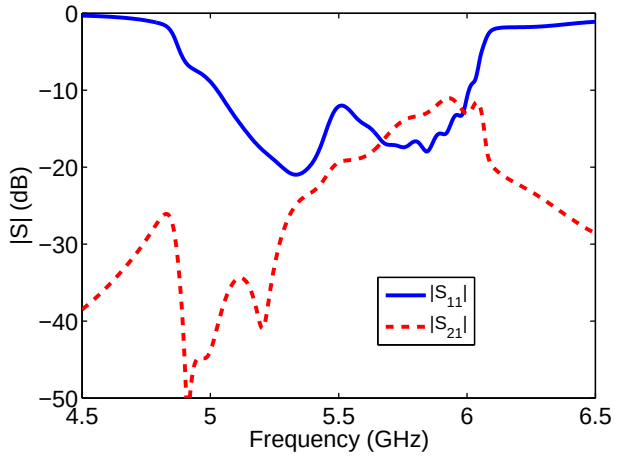

Fig. 7. Simulated S-parameters of the CRLH LWA in Fig. 6.

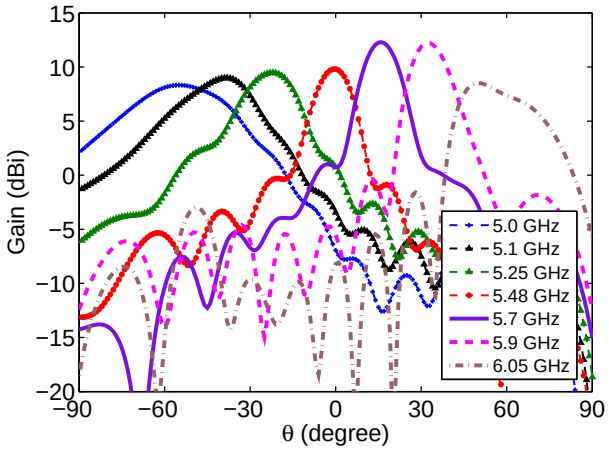

Fig. 8. Simulated x-z plane radiation patterns of the CRLH LWA in Fig. 6 at different frequencies.

permeability and the permeability of free space, respectively. The other parameters d, w, l, h and g are the via diameter, the width of a patch, the length of a patch, the thickness of a substrate and gap width, respectively. Note that International System of Units is employed in the above equations, i.e., the dimensions of the unit cell are in meter (m), and the values of the inductors and capacitors are in Henry (H) and Farad (F). Since the calculated values are approximate, especially for the outer patch in which a slot is present, we have done a slight adjustment to make the dispersion diagram closely similar to that from the eigenmode solver. The dispersion diagram for the equivalent circuit model is also plotted in Fig. 5 together with the one from CST. This study also verifies that higher values of the RH parameters and lower values of the LH parameters are required to achieve similar dispersion, i.e., a reduced frequency sweep.

B. Antenna Configuration

Figs. 6(a) and (b) show the top and perspective views of the CRLH LWA, respectively, designed using the unit cell discussed in Section III-A. A total of nine unit cells are used in the antenna design, considering the length and leakage rate of the antenna. This antenna is fed using a narrow uniform line and its dimensions are optimized to obtain good impedance matching. The length (l_{feed}) and width (w_{feed}) of the feed line are 13.25 and 1.7 mm, respectively. The length (L_{Ant}) of the complete structure is 252.75 mm, i.e., $4.62\lambda_0$, where λ_0 is calculated at 5.48 GHz. The frequency (5.48 GHz) chosen here is the transition frequency, i.e., the frequency when the main beam points at the broadside direction.

C. Scattering Parameters and Radiation Patterns

The simulated S-parameters and the x-z plane radiation patterns of the CRLH LWA in Fig. 6 are shown in Figs. 7 and 8, respectively. The beam points at $-55°$ at 5 GHz, and with an increase of frequency scans gradually towards the broadside ($0°$). For example, the radiation beam points at

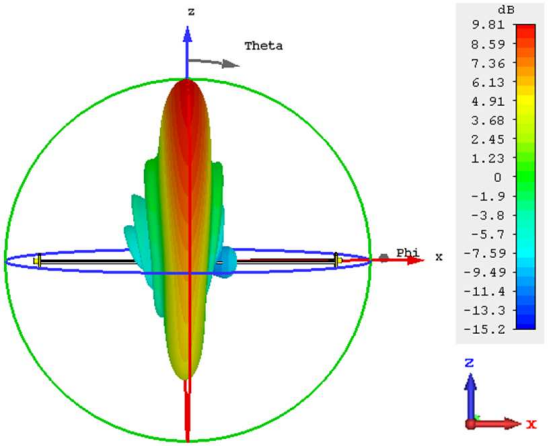

Fig. 9. Simulated 3D radiation pattern of the CRLH LWA in Fig. 6 when the beam points at the broadside direction.

$-38°$ and $-22°$ at 5.1 and 5.25 GHz, respectively. When the frequency increases further the beam scans through broadside to the forward direction. For instance, the main beam points at broadside ($0°$) at 5.48 GHz. For frequencies beyond 5.48 GHz the beam scans in the forward direction, e.g., the beam points at $+32°$ and $+50°$ at 5.9 and 6.05 GHz, respectively. The beamwidth is wide at a few frequency points compared to other beams. This is mainly due to a change of the effective antenna aperture with frequency which is explained further in Section III-D. For better representation a 3D radiation pattern of the broadside directed beam is shown in Fig. 9. It is clear that the antenna produces a fan-shaped beam, in which the beamwidth is narrow in the x-z plane and wide in the y-z plane. Finally, a comparison between the beam direction calculated from the unit cell dispersion diagram and full-wave simulation is shown in Fig. 10. A very good agreement can be observed between them. The slight variation between the full-wave simulation and the unit cell dispersion is due

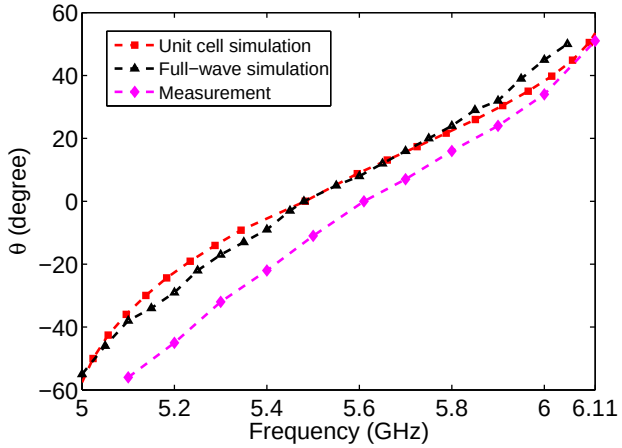

Fig. 10. Simulated and measured main beam direction as a function of frequency.

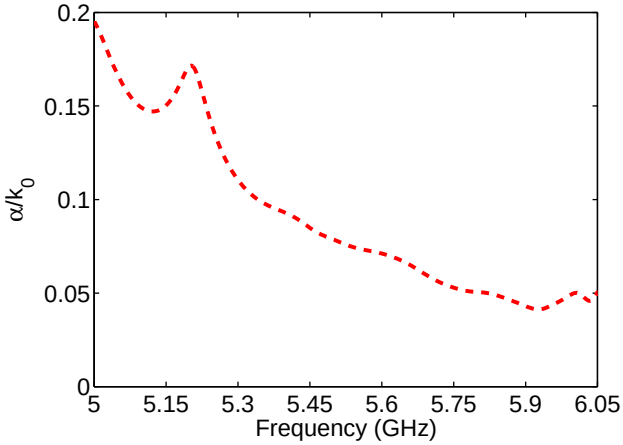

Fig. 12. Simulated leakage constant (α/k_0) of the CRLH LWA as a function of frequency.

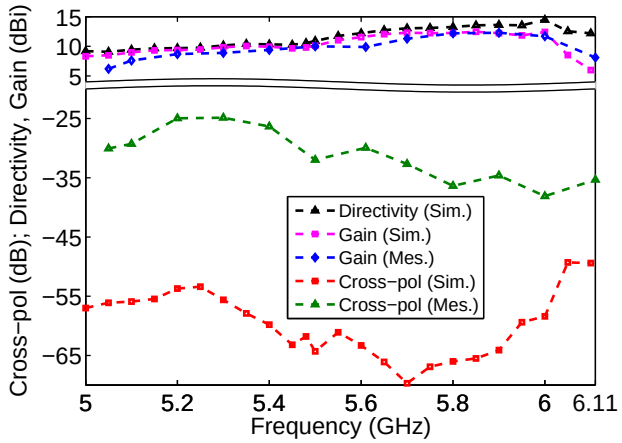

Fig. 11. Simulated gain, directivity and cross-pol and measured gain and cross-pol of the CRLH LWA in Fig. 6.

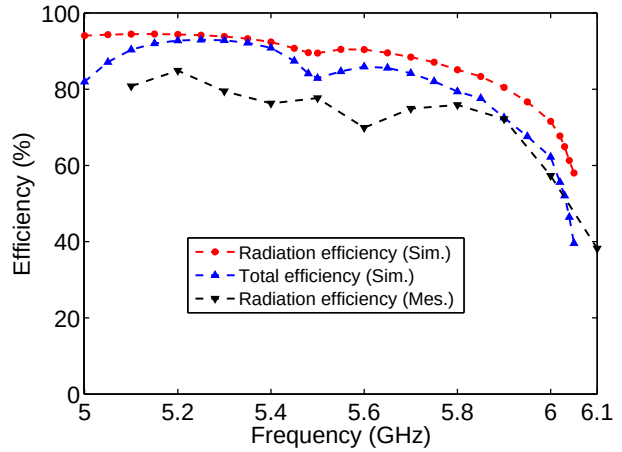

Fig. 13. Simulated radiation and total efficiencies and measured radiation efficiency of CRLH LWA.

to the fact that the dispersion diagram considers an infinite number of unit cells whereas our finite antenna is composed of only nine unit cells. The simulated cross-polarization level at different frequencies are shown in Fig. 11. Its value in the main beam directions remains below -49 dB throughout the beam scan range.

D. Leakage Rate

Fig. 12 shows the simulated leakage rate of the antenna as a function of frequency, calculated using the S-parameters of the whole structure. It can be seen that, at low frequencies, e.g. at 5 GHz, the leakage rate of the antenna is high. A higher leakage rate implies that, instead of the input power travelling towards the other end, it leaks or radiates quickly from a few unit cells at the left side of the antenna near the feed (Fig. 6), which results in a wider beam and consequently lower directivity and gain [7]. The leakage decreases with an increase of frequency, power leaks gradually and travels toward the load end, increases the effective aperture. As a result, the beamwidth decreases and the directivity increases. At higher frequencies, some of the power is absorbed by the load and hence the efficiency and gain degrades. The power absorption can be reduced by increasing the length of the antenna, but that will result in a long antenna structure.

E. Directivity, Gain and Efficiency

The simulated gain and directivity of the CRLH LWA are shown in Fig. 11. It is seen that the directivity and gain of the LWA are low at lower frequencies; for example the directivity and gain at 5 GHz are 9.19 and 8.33 dBi, respectively. Lower values of gain at lower frequencies, e.g., 8.5 dBi at 5.05 GHz, are due to the short effective aperture and wider beamwidth at those frequency points. However, the directivity and gain

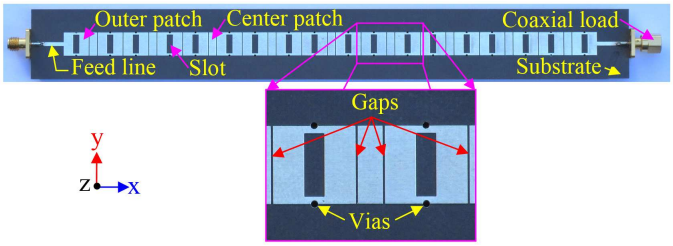

Fig. 14. Top view of the CRLH LWA prototype.

increase with frequency; the directivity and gain at 5.7 GHz are 13.05 and 12.3 dBi, respectively, and this is because of the long effective aperture at higher frequencies. When the frequency is very high the directivity decreases slightly, but the gain decreases significantly. The sudden decrement of antenna gain is due to the power absorbed by the load, as at these frequency points the energy travels to the other end and radiation occurs from all the unit cells in the antenna structure. As mentioned before, by using more unit cells the gain at high frequency points could be improved. The gain of the CRLH LWA is 8.52 dBi at 6.05 GHz.

Fig. 13 shows the simulated radiation (without mismatch losses) and total (with mismatch losses) efficiencies of the CRLH LWA in Fig. 6. It can be seen that the radiation efficiency of the antenna is high at lower frequencies, e.g., 94% at 5 GHz, and decreases gradually as frequency increases. For example, the radiation efficiencies are 90.4%, 80.5% and 58% at 5.6, 5.9 and 6.05 GHz, respectively. The total efficiency follows a similar trend to the radiation efficiency. However, the differences between the radiation and total efficiencies are more at 5 and 6.05 GHz. This is due to poor input impedance matching, as the total efficiency considers mismatch losses, at these frequency points. The total efficiency is >80% between 5 and 5.75 GHz.

F. Prototype and Measured Results

For further verification of the study we have fabricated and measured the CRLH LWA design in Fig. 6. Fig. 14 depicts the top view of the CRLH LWA prototype.

The measured (using an Agilent PNA-X N5242A Network Analyzer) S-parameters of the antenna prototype are shown in Fig. 15. There is a good agreement between the measured and simulated S-parameters except a negligible frequency shift. This might be due to minor fabrication errors. The CRLH LWA prototype has a -10 dB $|S_{11}|$ bandwidth of 5.14 - 6.1 GHz. For frequencies below 5.14 GHz $|S_{11}|$ is > -10 dB but remains <-7.47 dB for frequencies down to 5.1 GHz. The measured reflection coefficient of the antenna at 6.11 GHz is -9.32 dB. The measured transmission coefficient ($|S_{21}|$) of the antenna at 5.1 GHz is <-50 dB and increases gradually with frequency. The transmission coefficient decreases again for frequencies beyond 6.1 GHz. This happens because the reflection coefficient starts increasing beyond this frequency point.

Fig. 16 presents the measured radiation patterns of the

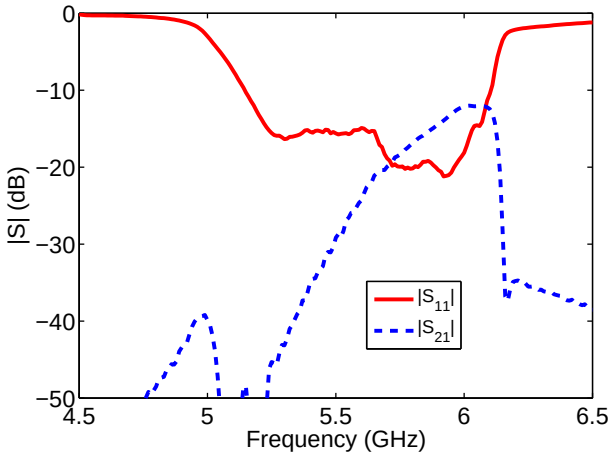

Fig. 15. Measured S-parameters of the CRLH LWA prototype in Fig. 14.

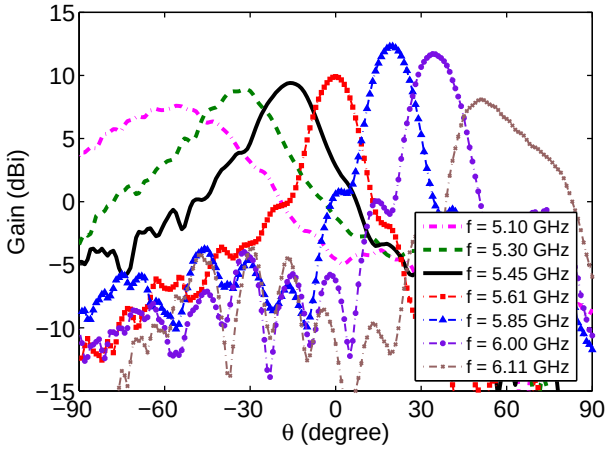

Fig. 16. Measured x-z plane radiation patterns of CRLH LWA prototype in Fig. 14 at seven frequency points.

CRLH LWA prototype at different frequencies. The main beam points at $-56°$ at 5.1 GHz, and with an increase of frequency gradually scans towards the broadside direction. The main beam points exactly at broadside at 5.61 GHz. At frequencies beyond 5.61 GHz the beam scans towards the forward direction. The beam points at $+34°$ and $+51°$ at 6 and 6.11 GHz, respectively. From the measured results we see that $-56°$ to $+51°$ of continuous beam scanning can be achieved by sweeping the frequency across a range of only 1.01 GHz. A comparison between the measured and simulated beam directions is shown in Fig. 10. In both cases the scan ranges are similar. However, the slight discrepancy between the measured and simulated beam directions is due to the frequency shift of the prototype compared to the simulated result as mentioned above. Fig. 17 shows the measured and simulated y-z-plane radiation patterns for the broadside beam. Again, a very good agreement is observed between them.

The measured gain of the CRLH LWA is shown in Fig. 11. A gain comparison method, using a standard gain horn antenna,

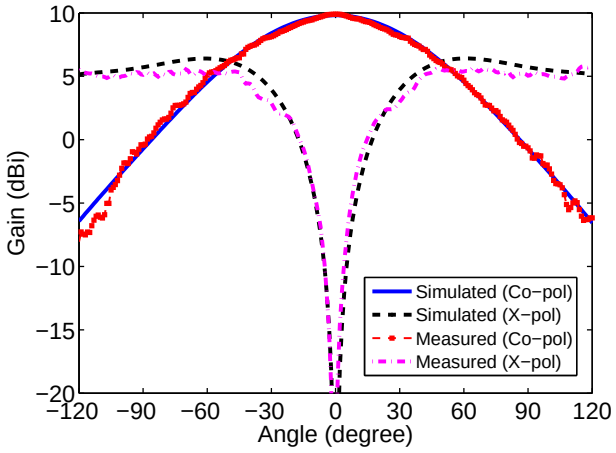

Fig. 17. Measured and simulated y-z plane radiation patterns of CRLH LWA when the main beam points at the broadside direction.

was used for gain measurement. The measured gain follows a similar trend to that of the simulated one, i.e., the gain is low at lower frequencies (7.6 dBi at 5.1 GHz) and increases (8.7 dBi at 5.2 GHz) with frequency. The maximum measured gain of the antenna is 12.3 dBi at 5.9 GHz and the gain is over 8 dBi within 5.2 - 6.11 GHz. The measured cross-polarization level of the antenna is also shown in Fig. 11. It can be seen that the measured cross-polarization level is always < -24.5 dB across the beam scan range. The measured radiation efficiency of the LWA prototype is shown in Fig. 13 together with the simulated results. The measured radiation efficiency has been calculated using the measured S-parameters, realized gain and directivity by the method described in [52]. Good agreement is observed between the simulated and measured results, although the measured results are slightly lower than the simulated ones.

IV. Discussion

An in-depth study on the equivalent circuit model of a CRLH LWA unit cell has been conducted to understand the main controlling parameters of the frequency range achievable for a wide-angle beam scan. It is shown that the range of the frequency sweep can be chosen flexibly. Since in real-world applications the frequency bands are usually predefined and in most cases the allocated frequency band for each application is narrow, we concentrated on reducing the frequency sweep range while maintaining a wide-angle beam scan. To verify our study, a novel CRLH LWA was designed and its performances were evaluated. The antenna needs a narrow range of frequency sweep to achieve a wide-angle beam scan. The narrowband CRLH LWA was fabricated and tested to verify our theory. It is noted that, although only one antenna configuration is discussed here, one can design a CRLH LWA with other antenna configurations for a desired frequency range by following the design guidelines in Section II. This study would be useful for CRLH LWA design with a targeted frequency range in future wireless systems or in beam-scanning applications.

We have controlled the frequency range while still achieving wide-angle scanning. It is relevant to compare our outcomes with a variety of previously reported results and this is shown in Table I. The performance of the prototype has been compared with not only CRLH antennas but also antennas which are capable of a continuous beam scan from backward to forward directions. It is seen that the proposed antenna requires a very limited frequency sweep for wide-angle beam scanning compared to the reference antennas listed in Table I.

TABLE I. Comparison Between the Proposed CRLH LWA with Limited Frequency Sweep and Backward-to-Forward Beam Scanning Reference LWAs.

Reference	Antenna Type	Frequency Sweep (FB)	Scan Range
[16]	Periodic CRE	(≈)12.5 - 19.45 GHz (43.5%)	-48° to $+35^\circ$
[17]	Periodic HW-MLWA	4.4 - 8.8 GHz (66.67%)	-54° to $+49^\circ$
[18]	Noncutoff SIW	9.0 - 14 GHz (43.48%)	-40° to $+35^\circ$
[19]	Dielectric image line	12 - 16.8 GHz (33.33%)	-65° to $+25^\circ$
[20]	Periodic SIW	7.625 - 11 GHz (36.24%)	-74° to $+45^\circ$
[21]	Half-mode periodic SIW	8.4 - 11.6 GHz (32.0%)	-43° to $+43^\circ$
[33]	NRI-TL supercell	4.9 - 7.7 GHz (44.44%)	-67° to $+58^\circ$
[34]	SIW-based CRLH	12 - 17 GHz (34.48%)	-62° to $+33^\circ$
[35]	Double Periodic CRLH	11.5 - 18 GHz (44.07%)	-42° to $+40^\circ$
[36]	Multilayered CRLH	8.25 - 13 GHz (44.7%)	-60° to $+66^\circ$
[37]	SIW-based CRLH	13.5 - 17.8 GHz (27.47%)	-57° to $+30^\circ$
[39]	Double layer Microstrip	4.1 - 6.1 GHz (39.22%)	-29° to $+72^\circ$
[40]	SIW-based CRLH	24 - 27 GHz (11.77%)	-17° to $+13^\circ$
[41]	Half-mode SIW	13.5 - 17.8 GHz (27.47%)	-66° to $+20^\circ$
[42]	Multilayered CRLH TL	20 - 30 GHz (40%)	-25° to $+50^\circ$
This work	Single layer CRLH LWA	5.1 - 6.11 GHz (18.02%)	-56° to $+51^\circ$

FB: fractional bandwidth; CRE: complementary radiation elements; HW-MLWA: half-width microstrip LWA; SIW: substrate integrated waveguide; NRI: negative-refractive-index; TL: transmission-line;

V. Conclusion

A method to achieve a desired frequency range flexibly and wide-angle scanning of CRLH LWAs is presented. The method is supported by a theoretical analysis, EM simulations and experiment. A novel narrowband CRLH LWA with a wide-angle beam scan is developed, analyzed and fabricated to verify the proposed concept. The measured results confirm that the CRLH LWA prototype is capable of scanning the beam continuously from -56° to $+51^\circ$ by sweeping the frequency from 5.1 to 6.11 GHz. A guideline is also outlined to design such LWAs for a targeted frequency band.

Acknowledgment

The authors would like to thank the reviewers for their valuable comments which have helped to improve this paper.

REFERENCES

[1] W. W. Hansen, "Radiating electromagnetic waveguide," U.S. Patent 2.402.622, 1940.

[2] L. Goldstone and A. A. Oliner, "Leaky-wave antennas I: rectangular waveguides," *IRE Trans. Antennas Propag.*, vol. 7, no. 4, pp. 307–319, Oct. 1959.

[3] R. Garg, K. C. Gupta, and R. Sharan, "A thin wall leaky waveguide antenna," *IEEE Trans. Antennas Propag.*, vol. 23, no. 1, pp. 107–112, Jan. 1975.

[4] W. Menzel, "A new travelling wave antenna in microstrip," in *Proc. 8th Eur. Microw. Conf.*, Sep. 1978, pp. 302–306.

[5] T.-L. Chen, Y.-D. Lin, and J.-W. Sheen, "Microstrip-fed microstrip second higher order leaky-mode antenna," *IEEE Trans. Antennas Propag.*, vol. 49, no. 6, pp. 855–857, Jun. 2001.

[6] Y. Geng, J. Wang, Y. Li, Z. Li, M. Chen, and Z. Zhang, "Leaky-wave antenna array with a power-recycling feeding network for radiation efficiency improvement," *IEEE Trans. Antennas Propag.*, vol. 65, no. 5, pp. 2689–2694, May 2017.

[7] D. K. Karmokar, K. P. Esselle, and T. S. Bird, "Wideband microstrip leaky-wave antennas with two symmetrical side beams for simultaneous dual-beam scanning," *IEEE Trans. Antennas Propag.*, vol. 64, no. 4, pp. 1262–1269, Apr. 2016.

[8] N. Nguyen-Trong, T. Kaufmann, L. Hall, and C. Fumeaux, "Optimization of leaky-wave antennas based on non-uniform HMSIW," in *Proc. IEEE MTT-S Int. Conf. NEMO*, Aug. 2015.

[9] Q. Lai, C. Fumeaux, and W. Hong, "Periodic leaky-wave antennas fed by a modified half-mode substrate integrated waveguide," *IET Microw., Antennas Propag.*, vol. 6, no. 5, pp. 594–601, Apr. 2012.

[10] D. K. Karmokar, Y. J. Guo, P. Y. Qin, K. P. Esselle, and T. S. Bird, "Forward and backward beam-scanning tri-band leaky-wave antenna," *IEEE Antennas Wireless Propag. Lett.*, vol. 16, pp. 1891–1894, 2017.

[11] M. Garcia-Vigueras, J. L. Gomez-Tornero, G. Goussetis, A. R. Weily, and Y. J. Guo, "Enhancing frequency-scanning response of leaky-wave antennas using high-impedance surfaces," *IEEE Antennas Wireless Propag. Lett.*, vol. 10, pp. 7–10, 2011.

[12] D. K. Karmokar and K. P. Esselle, "Periodic U-slot-loaded dual-band half-width microstrip leaky-wave antennas for forward and backward beam scanning," *IEEE Trans. Antennas Propag.*, vol. 63, no. 12, pp. 5372–5381, Dec. 2015.

[13] M. A. Antoniades and G. V. Eleftheriades, "A CPS leaky-wave antenna with reduced beam squinting using NRI-TL metamaterials," *IEEE Trans. Antennas Propag.*, vol. 56, no. 3, pp. 708–721, Mar. 2008.

[14] J. L. Gomez-Tornero, D. Caete-Rebenaque, and A. Alvarez-Melcon, "Microstrip leaky-wave antenna with control of leakage rate and only one main beam in the azimuthal plane," *IEEE Trans. Antennas Propag.*, vol. 56, no. 2, pp. 335–344, Feb. 2008.

[15] D. R. Jackson, C. Caloz, and T. Itoh, "Leaky-wave antennas," *Proc. IEEE*, vol. 100, no. 7, pp. 2194–2206, Jul. 2012.

[16] Y. L. Lyu, F. Y. Meng, G. H. Yang, Q. Wu, and K. Wu, "Leaky-wave antenna with alternately loaded complementary radiation elements," *IEEE Antennas Wireless Propag. Lett.*, vol. 17, no. 4, pp. 679–683, Apr. 2018.

[17] Y. Li, Q. Xue, H.-Z. Tan, and Y. Long, "The half-width microstrip leaky wave antenna with the periodic short circuits," *IEEE Trans. Antennas Propag.*, vol. 59, no. 9, pp. 3421–3423, Sep. 2011.

[18] Y. L. Lyu, X. X. Liu, P. Y. Wang, D. Erni, Q. Wu, C. Wang, N. Y. Kim, and F. Y. Meng, "Leaky-wave antennas based on noncutoff substrate integrated waveguide supporting beam scanning from backward to forward," *IEEE Trans. Antennas Propag.*, vol. 64, no. 6, pp. 2155–2164, Jun. 2016.

[19] C. S. Prasad and A. Biswas, "Dielectric image line-based leaky-wave antenna for wide range of beam scanning through broadside," *IEEE Trans. Antennas Propag.*, vol. 65, no. 8, pp. 4311–4315, Aug. 2017.

[20] D. K. Karmokar, Y. J. Guo, P. Y. Qin, S.-L. Chen, and T. S. Bird, "Substrate integrated waveguide-based periodic backward-to-forward scanning leaky-wave antenna with low cross-polarization," *IEEE Trans. Antennas Propag.*, vol. 66, no. 08, pp. 3846–3856, Aug. 2018.

[21] R. Henry and M. Okoniewski, "A broadside-scanning half-mode substrate integrated waveguide periodic leaky-wave antenna," *IEEE Antennas Wireless Propag. Lett.*, vol. 13, pp. 1429–1432, 2014.

[22] Y. Dong and T. Itoh, "Promising future of metamaterials," *IEEE Microw. Mag.*, vol. 13, no. 2, pp. 39–56, Mar. 2012.

[23] N. Engheta and E. R. W. Ziolkowski, *Metamaterials: Physics and Engineering Explorations*. New York: IEEE Press/Wiley, 2006.

[24] L. Liu, C. Caloz, and T. Itoh, "Dominant mode leaky-wave antenna with backfire-to-endfire scanning capability," *Electron. Lett.*, vol. 38, no. 23, pp. 1414–1416, Nov. 2002.

[25] E. F. Capolino, *Metamaterials Handbook: Applications of Metamaterials*. Boca Raton: FL: CRC Press, 2009.

[26] A. Lai, T. Itoh, and C. Caloz, "Composite right/left-handed transmission line metamaterials," *IEEE Microwave Mag.*, vol. 5, no. 3, pp. 34–50, Sept. 2004.

[27] G. V. Eleftheriades and E. K. G. Balmain, *Negative Refraction Metamaterials: Fundamental Principles and Applications*. New York: IEEE Press/Wiley, 2005.

[28] R. Marques, F. Martin, and M. Sorolla, *Metamaterials with Negative Parameters*. New York: Wiley, 2007.

[29] T. J. Cui, D. R. Smith, and E. R. Liu, *Metamaterials: Theory, Design, and Applications*. New York: Springer, 2010.

[30] F. Martin, *Artificial Transmission Lines for RF and Microwave Applications*. New York: Wiley, 2015.

[31] M. A. Antoniades, H. Mirzaei, and G. V. Eleftheriades, "Transmission-line based metamaterials in antenna engineering," in *Handbook of Antenna Technologies*. Singapore: Springer, 2016.

[32] M. Hashemi and T. Itoh, "Evolution of composite right/left-handed leaky-wave antennas," *Proc. IEEE*, vol. 99, no. 10, pp. 1746–1754, Oct. 2011.

[33] A. Mehdipour and G. V. Eleftheriades, "Leaky-wave antennas using negative-refractive-index transmission-line metamaterial supercells," *IEEE Trans. Antennas Propag.*, vol. 62, no. 8, pp. 3929–3942, Aug. 2014.

[34] C. Jin, A. Alphones, and L. C. Ong, "Broadband leaky-wave antenna based on composite right/left handed substrate integrated waveguide," *Electron. Lett.*, vol. 46, no. 24, pp. 1584–1585, Nov. 2010.

[35] C. Jin and A. Alphones, "Leaky-wave radiation behavior from a double periodic composite right/left-handed substrate integrated waveguide," *IEEE Trans. Antennas Propag.*, vol. 60, no. 4, pp. 1727–1735, Apr. 2012.

[36] Nasimuddin, Z. N. Chen, and X. Qing, "Substrate integrated metamaterial-based leaky-wave antenna with improved boresight radiation bandwidth," *IEEE Trans. Antennas Propag.*, vol. 61, no. 7, pp. 3451–3457, Jul. 2013.

[37] H. Zhang, Y. C. Jiao, G. Zhao, and C. Zhang, "CRLH-SIW-based leaky wave antenna with low cross-polarisation for Ku-band applications," *Electron. Lett.*, vol. 52, no. 17, pp. 1426–1428, 2016.

[38] Y. Mizumori, K. Okubo, M. Kishihara, J. Yamakita, and I. Ohta, "Backfire-to-endfire radiation characteristics of CRLH-TL using substrate integrated waveguide and metal-patches," in *Proc. Asia Pacific Microw. Conf.*, Dec. 2009, pp. 1419–1422.

[39] H.-X. Xu, G.-M. Wang, and M.-Q. Qi, "A leaky-wave antenna using double-layered metamaterial transmission line," *Applied Physics A*, vol. 111, no. 2, pp. 549–555, May 2013.

[40] W. Cao, Z. N. Chen, W. Hong, B. Zhang, and A. Liu, "A beam scanning leaky-wave slot antenna with enhanced scanning angle range and flat gain characteristic using composite phase-shifting transmission line," *IEEE Trans. Antennas Propag.*, vol. 62, no. 11, pp. 5871–5875, Nov. 2014.

[41] A. Sarkar, M. Adhikary, A. Sharma, A. Biswas, M. J. Akhtar, and Z. Hu, "Composite right/left-handed based compact and high gain leaky-wave antenna using complementary spiral resonator on HMSIW for Ku band applications," *IET Microw. Antennas Propag.*, vol. 12, no. 8, pp. 1310–1315, 2018.

[42] W. Jiang, C. Liu, B. Zhang, and W. Menzel, "K-band frequency-scanned leaky-wave antenna based on composite right/left-handed transmission lines," *IEEE Antennas Wireless Propag. Lett.*, vol. 12, pp. 1133–1136, 2013.

[43] J. M. Montero, A. M. Ocampo, and N. J. G. Fonseca, "C-band multiple beam antennas for communication satellites," *IEEE Trans. Antennas Propag.*, vol. 63, no. 4, pp. 1263–1275, Apr. 2015.

[44] Y. J. Guo, J. L. Gomez-Tornero, R. Guzman-Quiros, and A. R. Weily, "Reconfigurable leaky wave antennas," *Forum for Electromagnetic Research Methods and Application Technologies (FERMAT)*, vol. 1, pp. 1–11, 2014.

[45] L. Pazin and Y. Leviatan, "Narrow-size multiband inverted-F antenna," *IEEE Antennas Wireless Propag. Lett.*, vol. 10, pp. 139–142, 2011.

[46] C. Caloz and T. Itoh, *Electromagnetic Metamaterials: Transmission Line Theory and Microwave Applications*. New York: Wiley, 2005.

[47] D. M. Pozar, *Microwave Engineering*. 3rd ed., New York: Wiley, 2005.

[48] G. V. Eleftheriades, A. K. Iyer, and P. C. Kremer, "Planar negative refractive index media using periodically L-C loaded transmission lines," *IEEE Trans. Microw. Th. Tech.*, vol. 50, no. 12, pp. 2702–2712, Dec. 2002.

[49] H. Mosallaei and K. Sarabandi, "Design and modeling of patch antenna printed on magneto-dielectric embedded-circuit metasubstrate," *IEEE Trans. Antennas Propag.*, vol. 55, no. 1, pp. 45–52, Jan. 2007.

[50] H. W. Johnson and M. Graham, *High-speed digital design: a handbook of black magic*. Prentice Hall Upper Saddle River: Pearson Education (US), 1993.

[51] M. Kirschning, R. H. Jansen, and N. H. L. Koster, "Measurement and computer-aided modeling of microstrip discontinuities by an improved resonator method," in *Proc. IEEE MTT-S Int. Microw. Symp. Digest*, May 1983, pp. 495–497.

[52] C. A. Balanis, *Antenna Theory: Analysis and Design*. NY, USA: Wiley, 2005.

Debabrata K. Karmokar (S'12–M'15) received the B.Sc. degree in electrical & electronic engineering (EEE) from Khulna University of Engineering & Technology (KUET), Khulna, Bangladesh, in 2007 and the PhD degree in Electronic Engineering from Macquarie University, Sydney, NSW, Australia in 2015. He was an Assistant Professor and a member of Consultancy Research and Testing Services (CRTS) in the department of EEE, KUET, and an Assistant Director of Students' Welfare of the University. Between 2012 and 2015, he was a Research Assistant, a Casual Academic, and also a Secretary of the IEEE Student Branch, at Macquarie University. From 2016 to 2019 he was a Postdoctoral Research Associate with the Global Big Data Technologies Centre (GBDTC), University of Technology Sydney (UTS), Australia. He is currently a Lecturer with the School of Engineering, Macquarie University, Australia.

Dr. Karmokar is a recipient of several scholarships and awards including a District Council Scholarship from Satkhira District Council, Bangladesh, Technical Scholarship from KUET, a Commonwealth-funded International Postgraduate Research Scholarship (IPRS) together with an International Macquarie University Research Excellence Scholarship (iMQRES), an OCE PhD Scholarship from the Commonwealth Scientific and Industrial Research Organisation (CSIRO) ICT Centre, Marsfield, Australia, the First Prize in the Poster Competition at the Engineering Symposium 2015, Macquarie University, Young Scientist Award from Venus International Foundation in 2018, and URSI Young Scientist Award in 2019. He is serving as a reviewer for several journals of IEEE, IET, Wiley, Springer, MDPI, Hindawi and Elsevier etc.

Y. Jay Guo (Fellow'2014) received a Bachelor Degree and a Master Degree from Xidian University in 1982 and 1984, respectively, and a PhD Degree from Xian Jiaotong University in 1987, all in China. His research interest includes antennas, mm-wave and THz communications and sensing systems as well as big data technologies. He has published over 450 research papers including 220 journal papers and holds 26 patents in antennas and wireless systems. He is a Fellow of the Australian Academy of Engineering and Technology, a Fellow of IEEE and a Fellow of IET, and was a member of the College of Experts of Australian Research Council (ARC, 2016-2018). He has won a number of most prestigious Australian engineering and CSIRO awards, and was named one of the most influential engineers in Australia in 2014 and 2015, respectively.

Prof Guo is a Distinguished Professor and the founding Director of Global Big Data Technologies Centre (GBDTC) at the University of Technology Sydney (UTS), Australia. Prior to this appointment in 2014, he served as a Director in CSIRO for over nine years. Before joining CSIRO, he held various senior technology leadership positions in Fujitsu, Siemens and NEC in the U.K.

Prof Guo has chaired numerous international conferences. He is the Chair Elect of International Steering Committee, International Symposium on Antennas and Propagation (ISAP). He was the International Advisory Committee Chair of IEEE VTC2017, General Chair of ISAP2015, iWAT2014 and WPMC'2014, and TPC Chair of 2010 IEEE WCNC, and 2012 and 2007 IEEE ISCIT. He served as Guest Editor of special issues on "*Antennas for Satellite Communications*" and "*Antennas and Propagation Aspects of 60-90GHz Wireless Communications*," both in IEEE Transactions on Antennas and Propagation, Special Issue on "*Communications Challenges and Dynamics for Unmanned Autonomous Vehicles*," IEEE Journal on Selected Areas in Communications (JSAC), and Special Issue on "*5G for Mission Critical Machine Communications*", IEEE Network Magazine.

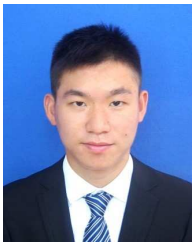

Shu-Lin Chen (S'16) was born in Hubei Province, China. He received the B.S. degree in electrical engineering from Fuzhou University, China, in 2012, and the M.S. degree in electromagnetic field and microwave technology from Xiamen University, China, in 2015. Since 2016, he has been working towards the PhD degree in Engineering with the Global Big Data Technologies Centre (GBDTC), University of Technology Sydney (UTS), Australia.

His research interests include reconfigurable antennas, leaky-wave antennas, millimeter wave antennas, and adaptive array processing. He was a finalist of ISAP 2017 best paper competition, and his paper was listed as an Honorary Mention in APS-URSI 2017.

Trevor S. Bird (S'71–M'76–SM'85–F'97-LF'15) received the B.App.Sc., M.App.Sc., and Ph.D. degrees from the University of Melbourne, Melbourne, VIC, Australia, in 1971, 1973, and 1977, respectively.

He was a Post-Doctoral Research Fellow with the Queen Mary College, University of London, London, U.K. He was a Lecturer with the Department of Electrical Engineering, James Cook University, Townsville, QLD, Australia. In 1983, he joined the Commonwealth Scientific and Industrial Research Organization, Sydney, NSW, Australia, where he held several positions, including the Chief Scientist of the ICT Centre, Marsfield, NSW. From 1982 to 1983, he was a Consultant with Plessey Radar, London. He is currently the Principal of Antengenuity, a specialist consulting firm, a Distinguished Visiting Professor with the University of Technology Sydney, Ultimo, NSW, and an Adjunct Professor with Macquarie University, North Ryde, NSW.

Dr. Bird is a Fellow of the Australian Academy of Technological and Engineering Sciences, the Institution of Electrical Technology (IET), the Royal Society of New South Wales, Queens College, University of Melbourne, and an Honorary Fellow of the Institution of Engineers, Australia. He was a member of the New South Wales Section Committee from 1995 to 2005, the Administrative Committee of the IEEE Antennas and Propagation Society from 2003 to 2005, the College of Experts of the Australian Research Council from 2006 to 2007, and the Technical Committee of numerous conferences, including JINA, ICAP, AP2000, IRMMW-THz, and the URSI Electromagnetic Theory Symposium. He was a Distinguished Lecturer for the IEEE Antennas and Propagation Society from 1997 to 1999, the Chair of the New South Wales Joint AP/MTT Chapter from 1995 to 1998, and again in 2003, the Chairman of the 2000 Asia Pacific Microwave Conference, and a Vice-Chair and the Chair of the Section from 1999 to 2000 and from 2001 to 2002, respectively. He was a recipient of the John Madsen Medal of the Institution of Engineers, Australia, on four occasions for the best paper published annually in the Journal of Electrical and Electronic Engineering, the CSIRO Medals for achievement in 1990, 1998, and 2011, the IEEE Third Millennium Medal for outstanding contributions to the IEEE New South Wales Section in 2000, several project awards from the Society of Satellite Professionals International (New York) in 2004, the Engineers Australia in 2001, and the Communications Research Laboratory, Japan, in 2000, the Centenary Medal for service to Australian society in telecommunications, the M.A. Sargent Medal in 2012 by Engineers Australia for sustained contributions to electrical engineering, and the James R. James Lifetime Achievement Award of IET in 2016 for outstanding contributions to the field of antennas and propagation. He was a co-recipient of the H.A. Wheeler Applications Prize Paper Award of the IEEE Antennas and Propagation Society in 2001. He was also named Professional Engineer of the Year by the Sydney Division, Engineers Australia in 2003. Since 2006, his biography has been listed in Who's Who in Australia. He was an Associate Editor of the IEEE TRANSACTIONS ON ANTENNAS AND PROPAGATION from 2001 to 2004, the Editor-in-Chief of the IEEE TRANSACTIONS ON ANTENNAS AND PROPAGATION from 2004 to 2010, and the President of the Society in 2013.